*Neuroscience* 134 (2005) 539–547

# CIRCADIAN AND LIGHT REGULATION OF OXYTOCIN AND PARVALBUMIN PROTEIN LEVELS IN THE CILIATED EPENDYMAL LAYER OF THE THIRD VENTRICLE IN THE C57 MOUSE

**K. DEVARAJAN[a], E. G. MARCHANT[b] AND B. RUSAK[a,c]***

[a]*Department of Psychology, Life Sciences Centre, Dalhousie University, Halifax, Nova Scotia, Canada B3H 4J1*

[b]*Department of Psychology, Malaspina University-College, Nanaimo, British Columbia, Canada V9R 5S5*

[c]*Departments of Psychiatry and Pharmacology, Dalhousie University, Halifax, Nova Scotia, Canada B3H 2E2*

**Abstract—The walls of the third ventricle have been proposed to serve as a bidirectional conduit for exchanges between the neural parenchyma and the cerebrospinal fluid. In immunohistochemical studies of mice, we observed that light exposure and circadian phase affected peptide staining surrounding the third ventricle at the level of the suprachiasmatic nuclei. Under high magnification, we observed robust staining for the neurohormone oxytocin and the calcium-binding protein parvalbumin associated with cilia extending into the third ventricle from the surrounding ventricular wall; no similar staining was observed for vasopressin or calbindin. Retinal illumination had opposite effects on levels of parvalbumin and oxytocin in the cilia: light exposure during late subjective night increased oxytocin staining, but decreased parvalbumin staining in the cilia. Preventing cellular transport with colchicine eliminated immunohistochemical staining for oxytocin in the cilia. There was also a significant daily rhythm of oxytocin immunostaining in the third ventricle wall, and in magnocellular neurons in the anterior hypothalamus. The results suggest that environmental lighting and circadian rhythms regulate levels of oxytocin in the cerebrospinal fluid, possibly by regulating movement of oxytocin through the third ventricle wall.** 

**Key words: circadian, immunohistochemistry, colchicine, entrainment, neurosecretion, immunofluorescence.**

The hypothalamic neuropeptide oxytocin (OXT) has been implicated in the regulation of social and reproductive behaviors, mood and stress responses in mammals (Gimpl and Farenholz, 2001; Insel et al., 2001; Porges, 2003; Razzoli et al., 2003; Winslow and Insel, 2004). Several of these behavioral systems are modulated by circadian (daily) rhythms and affected by ambient light exposure (Edery, 2001). The neural pathways by which these effects are mediated have not been described. The hypothalamic suprachiasmatic nucleus (SCN) at the base of the third ventricle (3V) functions as a pacemaker for circadian rhythms and its retinal input mediates synchronization (entrainment) of these rhythms to external lighting cycles (Rusak and Zucker, 1979; Moore, 1983; Meijer and Rietveld, 1989). Retinal input reaches the SCN but extends in some species to hypothalamic regions adjacent to the SCN where photically responsive neurons are also found (Johnson et al., 1988; Meijer et al., 1989).

Preliminary immunohistochemical studies of the distribution of OXT in C57Bl/6J mice indicated that it was not found in the SCN itself, while neural tissue surrounding the walls of the 3V at the level of the SCN showed high levels of OXT. Under higher magnification, OXT was detected immunohistochemically in association with cilia arising from ependymal cells in the 3V wall and protruding into the 3V.

The 3V wall likely plays an important role in regulating physiology and behavior by acting as a bi-directional conduit between the hypothalamus and the rest of the brain (Bruni et al., 1972, 1985; Bruni, 1974; Vigh and Vigh-Teichmann, 1992). The ventricular wall at the level of the SCN in the C57 mouse is lined with a layer of cuboidal ciliated ependymal cells (also called ependymocytes and periventricular epithelium) (Bruni, 1974; Bleier, 1975; Choudhury et al., 1979). The precise functions of these cilia are unknown; however, putative roles include moving cerebrospinal fluid (CSF), filtering debris, and mediating neurohormonal release/absorption via the CSF (Bruni et al., 1985). Because hormone release depends on calcium levels (Muschol and Salzberg, 2000; Egli et al., 2004; Li and Stern, 2004; Watanabe et al., 2004), we also investigated the localization of calcium-binding proteins (parvalbumin and calbindin) that might play a role in regulating OXT release.

The ependymal layer includes specialized ependymal cells called tanycytes, characterized by long basal processes that contact neurons and the cerebral vasculature (Altman and Bayer, 1978; Luiten et al., 1980; Akmayev and Popov, 1977; Millhouse, 1971). Below this layer is the subependymal layer containing glia and a dense neural plexus including a number of neuropeptide-containing processes that project to the CSF, the hypothalamus and the brain stem (Lorez and Richards, 1982; Chung and Lee, 1988; Choudhury and Ray, 1990; Ju et al., 1992; Cloft and Mitchell, 1994; Larsen et al., 1996; Vigh and Vigh-Teichmann, 1998).

*Correspondence to: B. Rusak, Department of Psychology, Life Sciences Centre, Dalhousie University, Halifax, Nova Scotia, Canada B3H 4J1. Tel: +1-902-494-2159; fax: +1-902-494-6585.
E-mail address: rusak@dal.ca (B. Rusak).

*Abbreviations:* AH, anterior hypothalamus; CSF, cerebrospinal fluid; DAB, diaminobenzidine; EM, electron microscope; LP, light pulse; NL, no light; OXT, oxytocin; PBS, phosphate-buffered saline; PVN, paraventricular nucleus of the hypothalamus; SCN, suprachiasmatic nucleus; S.E.M., standard error of the mean; VP, vasopressin; ZT, zeitgeber time; 3V, third ventricle.

0306-4522/05$30.00+0.00 
doi:10.1016/j.neuroscience.2005.04.034

We conducted immunohistochemical studies to investigate the regulation of parvalbumin and OXT levels within 3V cilia in response to retinal light exposure during mid-subjective day (zeitgeber time [ZT]8, with ZT0 defined as the beginning of the daily 12 h light phase) and late subjective night (ZT23) in the C57 mouse. These times were selected to represent contrasting responses of the circadian system to light input in mice: at ZT8, light does not shift circadian rhythms, while at ZT23, it causes very large shifts (advances) of these rhythms (Daan and Pittendrigh, 1976). OXT immunoreactivity was also measured in magnocellular neurons in the anterior hypothalamic area (AH) and in the paraventricular nuclei of the hypothalamus (PVN) (experiment 1). We also examined both OXT and parvalbumin immunostaining in the 3V wall, PVN and AH at six phases of the daily cycle in the absence of light exposure to evaluate whether their levels showed spontaneous daily rhythmicity (experiment 2). OXT immunostaining in cilia and magnocellular neurons in the PVN and AH area were also measured 24 h after central administration of colchicine to determine whether staining in the 3V cilia depends on active cellular transport mechanisms (experiment 3).

## EXPERIMENTAL PROCEDURES

### General methods

Male C57Bl/6J mice weighing 20–25 g were obtained from Charles River Laboratories Inc. (Montréal, Quebec, Canada), and housed in standard shoebox cages. All animals were maintained in a 12-h light/dark cycle (~300 lux in the light phase) for at least 4 weeks prior to any manipulations. Manipulations in darkness were carried out using infrared viewers (NVS 300-Powerplus Goggle with Illuminator, Kennesaw, GA, USA). Animals were killed with an overdose of sodium pentobarbital; once deeply anesthetized in darkness, their eyes were covered with black electrical tape and they were transported in the dark to the perfusion area. All procedures involving animals were conducted in accordance with the regulations of the Canadian Council on Animal Care and were approved by the Dalhousie University Committee on Laboratory Animals. All experiments in this study conformed to international guidelines on the ethical use of animals and care was taken to minimize the suffering and number of animals used.

### Procedures

*Experiment 1.* A total of 20 mice ($n=5$ per group) were used in this experiment. Animals were killed at either ZT8 or ZT23 with a barbiturate overdose; lights were not turned on as scheduled at ZT0 for the animals killed at ZT8. Light-exposed animals first received 30 min light pulses (LP) (300 lux) beginning at either ZT7 or ZT22, were then returned to darkness for a further 30 min and were killed in darkness at the same times as the animals that were not exposed to light. Thus, all animals were killed under identical conditions of darkness at both daily phases, with half having been exposed to light for 30 min beginning 60 min earlier (groups LP8 and LP23), and half not having any light exposure (groups no light (NL)8 and NL23). Brains were removed after perfusion, sectioned in a cryostat and prepared for immunohistochemical analysis of OXT and parvalbumin. To assess the specificity of the effects observed for these peptides, alternate sections were stained for the neuropeptide vasopressin (VP) or the calcium-binding protein calbindin (see below).

*Experiment 2.* Thirty-six mice were used in this experiment. Animals were housed as described above and six mice were killed at each of six times (ZT0, 4, 8, 12, 16, and 20). The lights did not come on as usual at ZT0 on the day of manipulation, so all animals were killed in the dark, and their brains were prepared for immunohistochemical studies. Unfrozen brains were sectioned through the hypothalamic region using a vibratome, because fresh sections yielded stronger OXT immunoreactivity than frozen sections. Vibratome sections, however, damaged the cilia lining the 3V, so analyses of daily rhythms in OXT immunoreactivity in this study were restricted to hypothalamic structures, excluding the cilia.

*Experiment 3.* To assess whether cellular transport is required for the appearance of OXT immunoreactivity in 3V cilia, male mice housed as described above were pretreated with i.c.v. injections of colchicine, which prevents microtubule-based transport. The mice were anesthetized with a ketamine/xylazine cocktail (200/10 mg/kg), mounted in a stereotaxic device, and injected into each lateral ventricle with 7.5 μg colchicine/2.5 μl saline or saline vehicle ($n=9$ per group) at the following coordinates: 0.2 mm caudal to bregma, ±1.2 mm lateral to the midline, and 2.5 mm ventral to the skull surface. Mice were deeply anesthetized 24 h later at ZT8 in normal lighting during their daily light phase. The brains were prepared for immunohistochemical studies, as described below. OXT immunoreactivity in all regions was analyzed using tissue sectioned in a cryostat in order to preserve the cilia intact.

### Immunohistochemistry

After full anesthesia, animals were perfused transcardially with physiological saline followed by 4% paraformaldehyde in 0.1 M phosphate buffer solution. Brains were extracted and post-fixed overnight at 4 °C in the same solution. Brains prepared for sectioning on the vibratome were cut in 30 μm coronal sections through the suprachiasmatic region. Brains prepared for sectioning on the cryostat were transferred to a phosphate buffer solution containing 30% sucrose and again stored at 4 °C. After 48 h, the brains were frozen (−18 °C) and 30 μm coronal sections were cut through the suprachiasmatic region. For both cryostat and vibratome brains, four series were collected in 0.01 M phosphate-buffered saline (PBS) with 0.05% sodium azide. Free-floating tissue sections were batch processed and stained immunohistochemically using the ABC technique (Hsu et al., 1981). Biotin-labeled secondary antibodies were of either goat or rabbit origin (Vector Laboratories, Burlingame, CA, USA).

After treatment in PBS with 3% hydrogen peroxide, tissue was incubated with the primary antibody (1:1000, see below) for 2 days with 0.3% Triton X-100 and 3% normal serum (Vector Laboratories). Sections were rinsed and incubated in biotin-conjugated secondary for 90 min. After additional rinsing, tissue was incubated in avidin–biotin complex (Vector Laboratories) for 90 min before being rinsed and developed with diaminobenzidine (DAB) as a chromogen (10 mg in 100 ml 0.1 M PB, pH 7.4). Immunofluorescence was used because it was more sensitive for labeling the parvalbumin antibody and because it allowed double-labeling using immunofluorescence for parvalbumin and DAB labeling for OXT. All immunofluorescent studies used exposure to Cy3-labeled streptavidin (Jackson Immunoresearch, West Grove, PA, USA) for 120 min following secondary antibody incubation.

OXT (Cat. No. HC 8152) and VP (Cat. No. IHC 8130) antisera (Peninsula Laboratories, Belmont, CA, USA) were raised in rabbit and are reported to be 100% reactive to human, bovine, porcine, sheep, rat and mouse OXT and VP, respectively. Parvalbumin antiserum (Cat. No. SC 7446, Santa Cruz Biotechnology Inc., Santa Cruz, CA, USA) was raised in goat and is reactive with rat and human parvalbumin. Mouse parvalbumin differs from human parvalbumin by only one amino acid. Calbindin antiserum (Cat.

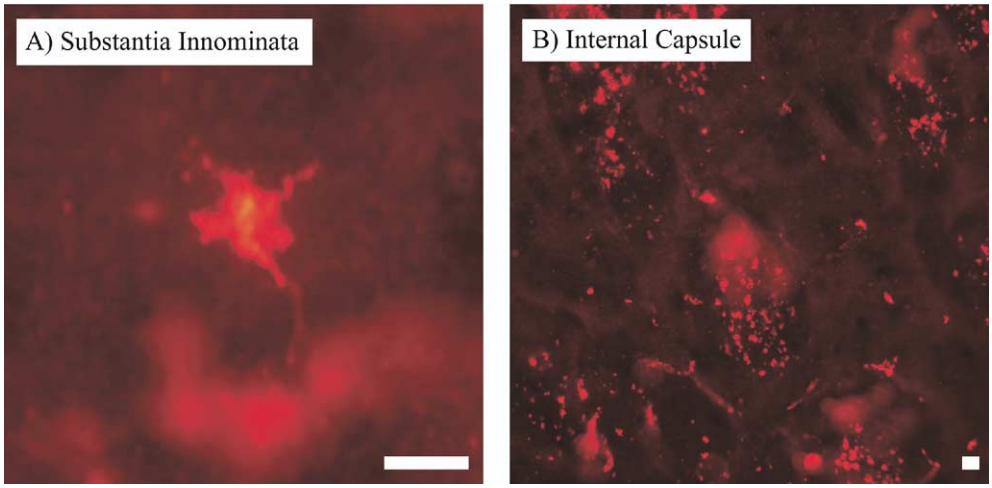


**Fig. 1.** Examples of known parvlabumin-immunoreactive tissues in the mouse. (A) A parvalbumin-immunoreactive neuron in the substantia innominata. (B) Parvalbumin staining in transected corticospinal axons descending through the internal capsule. Both sections show immunohistochemical staining of parvalbumin using Cy3-labeled streptavidin; they were taken from a mouse killed without light exposure during the subjective day at ZT8. Scale bar=0.01 mm.

No. AB 1778, Chemicon International Inc., Temecula, CA, USA) is reactive to human, rat and mouse calbindin.

Control procedures included omitting the primary antibody, followed by incubation in goat anti-rabbit serum and development with DAB for one set of tissue. Two other sets of tissue were processed omitting the primary antibody and were incubated in rabbit anti-goat serum. One of these sets was developed in DAB and the other was incubated in Cy3 streptavidin and processed for immunofluorescence. Another control set of tissue was processed by first blocking the OXT antibody with OXT peptide (Peninsula; 1:200). These measures were taken to assess non-specific staining, and no tissue staining was observed in the hypothalamus or cilia in any of these control series, although the unstained cilia were clearly visible at high magnification. To check on the reliability of the apparent parvalbumin staining in the cilia, we also examined brain regions previously reported to be immunoreactive for parvalbumin and confirmed that these regions also showed specific staining using these procedures (Fig. 1).

### Quantification and analysis

Microscopic images were captured using a digital Olympus C3030 or COHU CCD camera on a Zeiss Axioplan-II fluorescence microscope or an Olympus BH-2 microscope. All image analyses were carried out on unprocessed images using Scion Image software (version 1.62c). To measure parvalbumin immunoreactivity in the 3V cilia, an oval template was drawn around the bottom one-third of the 3V (area=58,555 square pixels). Care was taken to include only cilia while excluding the supraependymal layers. The area and density of parvalbumin immunofluorescence (Cy3) were measured on individual cilia in sections adjacent to the mid-section of the SCN (Fig. 2A and C). The mean density and the immunoreactive area of each cilium within this template were measured, multiplied together, and the product was averaged over three sections containing the SCN from each animal.

To measure OXT immunoreactivity in the cilia, a rectangular template (165×300 pixels) was placed over a collection of cilia on the inside of the 3V adjacent to the SCN. The mean density and the immunoreactive area of each cilium within this template were measured, multiplied together, and the product was averaged over three sections containing the SCN from each animal. To assess OXT immunoreactivity within the neural plexus surrounding the 3V, a template (30×100 pixels) was placed over the ventricle wall at the level of the SCN in one section from each animal, and the area of staining and average immunoreactive density within the template region were measured.

To assess OXT immunoreactivity in PVN and 3V/AH magnocellular neurons, a single section was selected for each of six (experiment 2) or nine (experiment 3) animals per group. The 3V/AH cells were measured within a template region in a section containing the SCN, while the PVN region was selected to include its distinct triangular shape at the dorsal edge of the 3V. Within the template region, the area and average density of labeling in each OXT-positive cell were measured and these values were multiplied to estimate the level of OXT staining.

All statistical analyses involved either a Student's *t*-test or a two-way analysis of variance with Tukey's HSD post hoc analysis (with Bonferroni correction for multiple comparisons). Results are presented as the mean±standard error of the mean (S.E.M.) and group differences are considered statistically significant when $P<0.05$. All measurements were carried out independently using coded sections by two experimenters who were blinded with respect to treatment condition. Inter-rater reliability was assessed in experiment 1 on measurements made by the two experimenters. For parvalbumin and OXT immunoreactivity in the cilia, the resulting Pearson correlation coefficients were 0.89 and 0.86, respectively. A similar correlation analysis on measurements taken from the PVN and 3V/AH area for the two raters resulted in coefficients of 0.92 and 0.94.

## RESULTS

### Experiment 1

We observed OXT-positive perikarya and fibers in the neural plexus surrounding the 3V of C57 mice, as has been reported previously in rats (Ju et al., 1992; Gimpl and Farenholz, 2001). We also observed parvalbumin immunoreactivity in the neural plexus and 3V wall of mice (Fig. 2), which is consistent with previous evidence of parvalbumin in the ependymal cells of rats (Celio, 1990). Cilia lining the 3V wall were also found to be immunoreactive for both parvalbumin and OXT, and this immunoreactivity was regulated by retinal illumination.

Parvalbumin was characteristically observed in discrete patches along the length of the cilia (Fig. 2A, 2C),

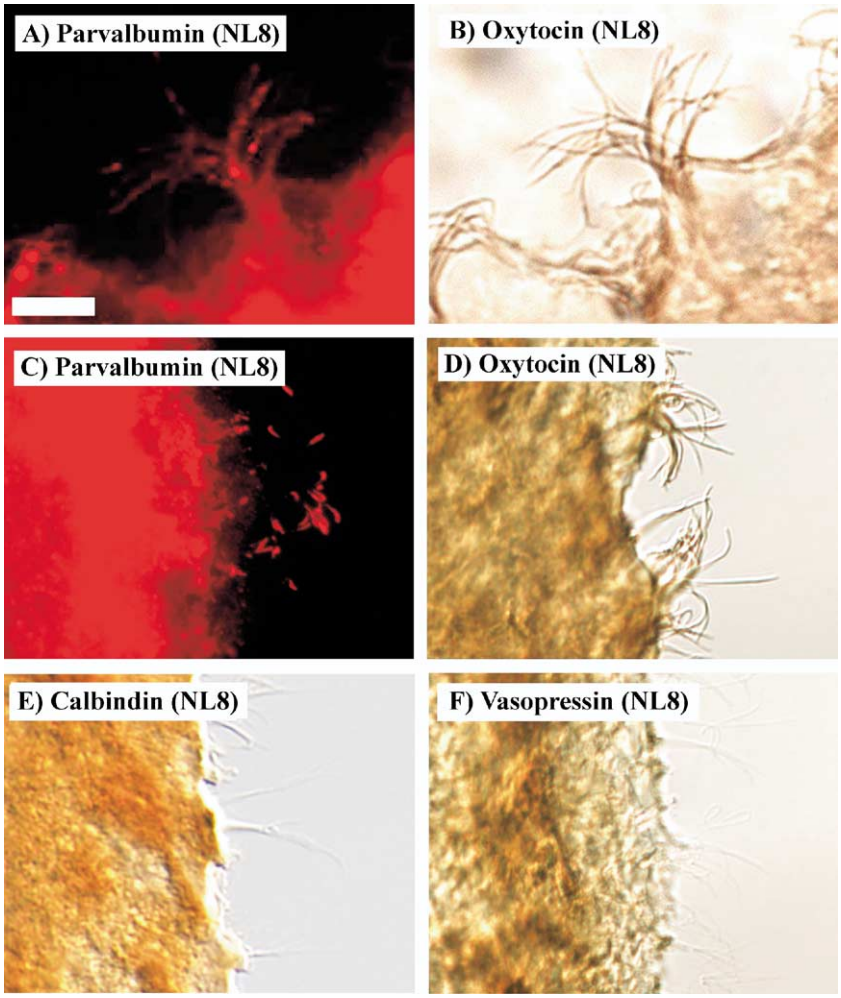


**Fig. 2.** Immunohistochemical staining in the lining of the 3V wall in mice. (A) Parvalbumin immunoreactivity, revealed using Cy3-labeled streptavidin, is shown in discrete patches along the length of cilia from the base of the 3V. In contrast, OXT immunoreactivity (B) appears along the full length of the cilia at the same level. Cilia from approximately mid-height of the 3V stained similarly for parvalbumin (C) and OXT (D) are also illustrated. When tissue was reacted for calbindin (E) or vasopressin (F) immunoreactivity, 3V cilia (mid-height) were not stained and are virtually translucent, despite robust staining in the adjacent ventricular wall. All animals were killed without light exposure during the subjective day at ZT8. Scale bar=0.01 mm, applies to all panels.

while OXT appeared to be distributed more uniformly over the length of the cilia (Fig. 2B, 2D). Parvalbumin protein levels (immunofluorescent area×density, measured in arbitrary units using Scion Image) in the 3V cilia were significantly decreased by a 30 min LP at ZT23 (20,013±720 vs. 17,024±884; $t_{(17)}=-2.54$, $P<0.05$), but not at ZT8 (Fig. 2A). Baseline parvalbumin protein levels measured from animals not exposed to LP were significantly higher at ZT23 compared with ZT8 (20,013±720 vs. 16,523±682, respectively, $t_{(11)}=3.46$, $P<0.05$). In the neural plexus surrounding the 3V wall, however, there were no significant differences observed in parvalbumin immunofluorescence in relation to either time or light exposure.

There was a significant interaction between time and light exposure for OXT immunoreactivity in the cilia ($F_{(1,18)}=8.98$, $P<0.01$). Tukey's HSD test revealed that light exposure increased OXT immunoreactivity (area× density) significantly in 3V cilia at ZT23 ($t_{(8)}=-2.35$, $P<0.05$; Fig. 2B), while the change in OXT levels at ZT8 was not statistically significant ($t_{(8)}=-1.93$, $P<0.09$). Significant differences were found in baseline immunoreactivity in the control animals, with higher levels being observed in the cilia at ZT8 than ZT23 in the absence of light ($t_{(8)}=3.46$, $P<0.01$; Fig. 3B).

In the neural plexus surrounding the 3V, the only significant difference observed was a higher density of OXT immunoreactivity in animals killed at ZT23 than at ZT8, after exposure to light ($t_{(17)}=2.56$, $P<0.05$; Fig. 4A). There were significant main effects of time ($F_{(1,17)}=8.42$, $P<0.05$) and light exposure ($F_{(1,17)}=12.04$, $P<0.01$) on OXT immunoreactivity in 3V/AH magnocellular neurons (Fig. 4B). OXT immunoreactivity was higher in the 3V/AH after light exposure at ZT23 than after light exposure at ZT8, and light exposure increased OXT immunoreactivity at ZT23 over levels in darkness. No significant main effects were found of time ($F_{(1,15)}=3.89$, $P<0.069$) or light ($F_{(1,15)}=0.94$, $P<0.34$) on OXT immunoreactivity in the PVN.

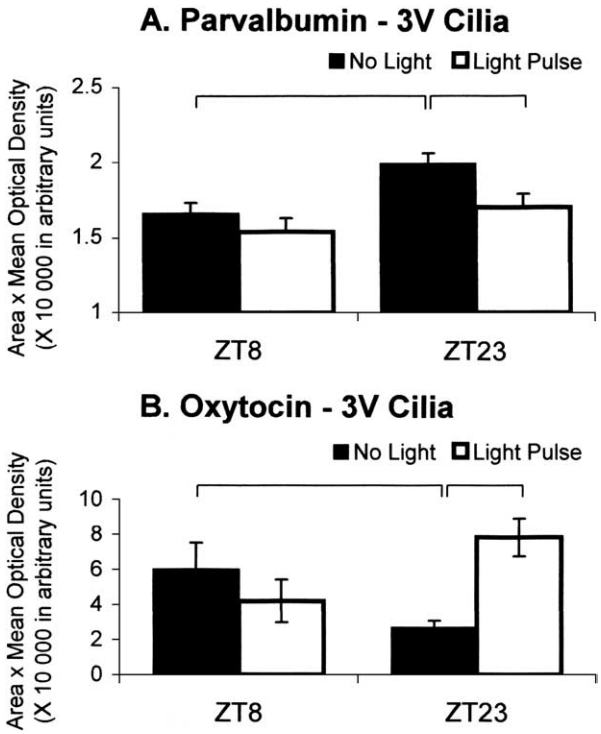


**Fig. 3.** (A) Parvalbumin immunofluorescent mean optical density×area in 3V cilia (mean±S.E.M.). Groups that differed significantly are connected by a horizontal line with vertical tick marks indicating the relevant groups. Baseline levels of parvalbumin immunoreactivity were significantly higher in the absence of light at ZT23 compared with ZT8 ($P<0.05$). Light caused a significant decrease in parvalbumin immunofluorescence in the cilia in late subjective night (ZT23, light vs. no light; $P<0.05$) but not in the subjective day (ZT8). (B) Oxytocin immunohistochemical mean optical density×area in 3V cilia (mean± S.E.M.). Oxytocin levels were significantly higher at ZT8 than ZT23 in the absence of light exposure ($P<0.05$). Light caused a significant increase in oxytocin staining in the cilia at ZT23 ($P<0.05$, light vs. no light), but no significant change at ZT8 ($P=0.09$).

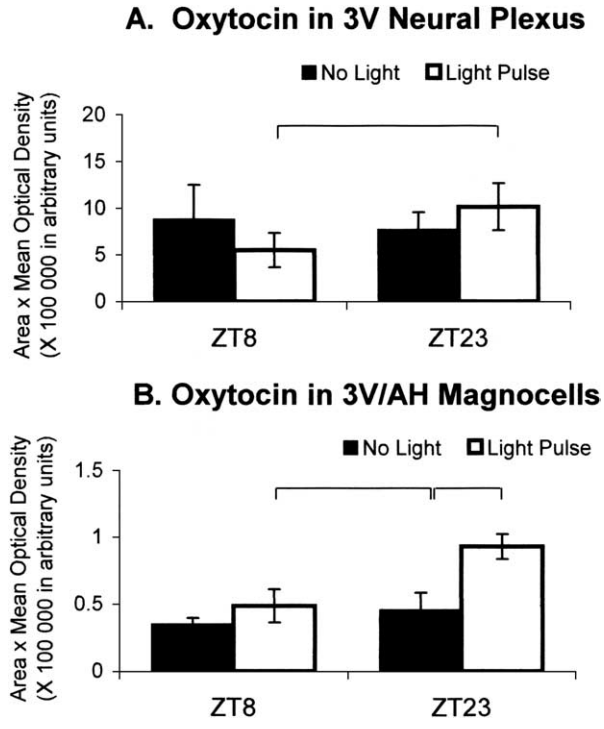


**Fig. 4.** Mean (±S.E.M.) oxytocin immunoreactive density in (A) the 3V neural plexus and (B) magnocellular neurons in the 3V/AH area. Groups that differed significantly are connected by a horizontal line with vertical tick marks indicating the relevant groups. (A) There was a significantly higher density of oxytocin staining in the neural plexus of animals exposed to light and killed at ZT23 than at ZT8 ($P<0.05$) (B) Oxytocin immunoreactivity in 3V/AH magnocellular neurons was increased significantly following light exposure at ZT23 ($P<0.05$), but not at ZT8 in the anterior hypothalamus (3V/AH). Oxytocin staining was also significantly higher in animals exposed to light and killed at ZT23 than at ZT8 ($P<0.05$).

There was no immunostaining visible in the cilia for either VP or calbindin under any conditions, despite staining for these peptides in the adjacent hypothalamus (Fig. 2E, 2F).

### Experiment 2

There were significant differences in OXT immunoreactivity (area×density) among circadian phases sampled in magnocellular neurons located in both the PVN ($F_{(5,30)}=21.55$, $P<0.0001$; Fig. 5A) and 3V/AH ($F_{(5,31)}=15.48$, $P<0.001$; Fig. 5B), and in the neural plexus surrounding the 3V wall ($F_{(5,30)}=6.07$, $P<0.001$; Fig. 5C). In all areas, staining was minimal in the early subjective day and peaked in the subjective night. Peak immunoreactivity was found at ZT16 in all three regions, while lowest values were found at ZT0 in the neural plexus, and at ZT4 in the PVN and 3V/AH area. Post hoc analyses with Bonferroni correction ($\alpha=0.0034$) revealed significant differences in immunoreactive density×area values among some of the ZTs tested. In the PVN, the value at ZT4 was significantly lower than those at ZT12 and ZT16, while the value at ZT20 was also significantly lower than that at ZT16 (Fig. 5A). In the 3V/AH area, ZT0 and ZT4 were both significantly lower than ZT16 (Fig. 5B). In the neural plexus, ZT0 was significantly lower than ZT12, ZT16 and ZT20, while ZT4 was significantly lower than ZT12 and ZT16 (Fig. 5C).

### Experiment 3

Colchicine pre-treatment 24 h earlier completely eliminated OXT immunoreactivity in 3V cilia at ZT8 (Fig. 6B), while saline controls had measurable amounts in their cilia (Fig. 6A). Since cilia were not visible in the colchicine-treated mice, their immunoreactivity could not be measured and no statistical assessment of the stark differences observed was necessary.

Despite processing all sections in a single batch, the background staining of colchicine-pretreated tissue appeared darker than control tissue. Previous studies have shown that colchicine can induce peptide gene expression in previously non-secretory neurons (Leah et al., 1993; Ekblad et al., 1996; Cougnon-Aptel et al., 1999). The apparent increase in background staining may therefore reflect a non-specific increase in OXT levels. The complete loss of OXT immunoreactivity associated with the cilia after

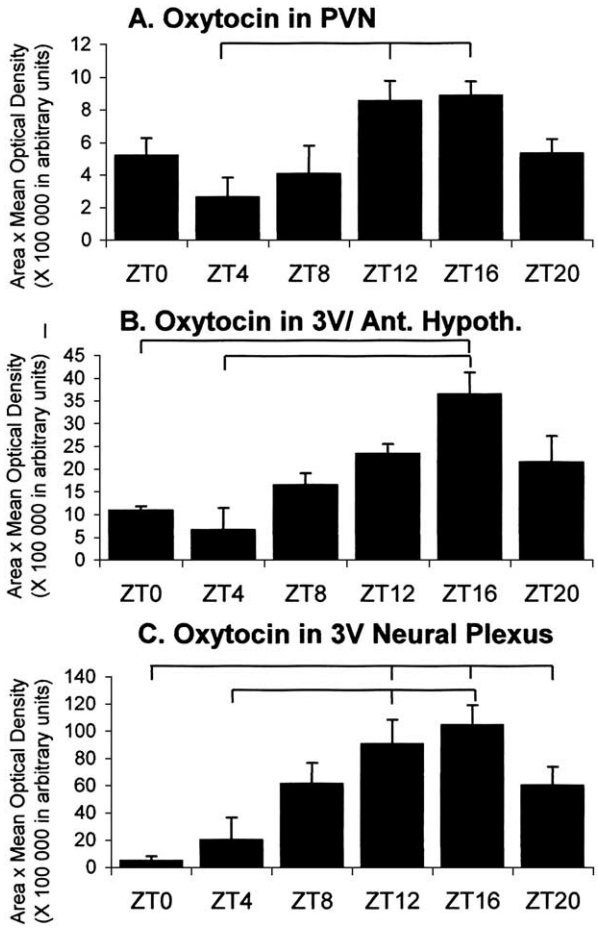


**Fig. 5.** Significant daily rhythms ($P<0.001$ in each case) of oxytocin immunoreactivity (density×area, measured at six daily phases in mice housed in darkness for 24 h) were found in the PVN (A), anterior hypothalamus (3V/AH) (B), and in the neural plexus surrounding the third ventricle (C). Groups that differed significantly are connected by a horizontal line with vertical tick marks indicating the relevant groups. Peak values were at ZT16 in each area and lowest values were at ZT0 or ZT4. (A) The value at ZT4 was significantly lower ($P<0.0034$, with a Bonferroni correction for multiple comparisons) from values at ZT12 and ZT16. The value at ZT20 was also significantly lower than that at ZT16. (B) Values at ZT0 and ZT4 were significantly lower than the value at ZT16. (C) The value at ZT0 was significantly lower than those at ZT12, ZT16 and ZT20, while that at ZT4 was significantly lower than those at ZT12 and ZT16.

colchicine treatment, even in the face of increased background staining, however, is strong evidence that the source of OXT is extrinsic to the cilia and that microtubule-based transport is necessary for cilia to be immunoreactive for OXT.

## DISCUSSION

Cilia lining the anterior hypothalamic walls of the 3V in C57 mice are immunoreactive for the neuropeptide OXT and the calcium-binding protein parvalbumin. There are also significant daily rhythms of OXT immunoreactivity in the PVN, 3V/AH magnocellular neurons and the neural plexus surrounding the 3V wall. Colchicine pretreatment eliminated OXT immunoreactivity from the cilia, suggesting that OXT observed in the cilia is actively transported from cells elsewhere, perhaps in the hypothalamus.

Parvalbumin immunoreactivity has been identified within neurons in many parts of the mammalian nervous system (Gaykema and Zaborszky, 1997; Zahm et al., 2003; see Fig. 1). It is unclear, however, whether parvalbumin and OXT are found within 3V cilia or attached to the surface of the cilia. Preliminary electron microscope (EM) studies (unpublished observations) suggest that these cilia show the same microtubule arrangement characteristic of cilia elsewhere in the body (Aughsteen, 2001). Since microtubule-based transport is required to observer OXT associated with cilia, and since OXT is reportedly synthesized in PVN neurons (Gimpl and Farenholz, 2001), it is possible that OXT is transported to the 3V wall and released into the ventricular CSF, where it contacts the cilia. The cilia may aid in distribution and movement of OXT into the 3V by their presumed fanning motion, or through a molecular transport mechanism, or both.

A transporter molecule (transthyretin) has been described on 3V cilia that may help transport thyroxine along the cilia (Kuchler-Bopp et al., 1998). It is possible that there is a similar molecular mechanism for holding and transporting OXT along the outside of the cilia, which would account for the intense OXT immunoreactivity of the cilia. Immunohistochemical studies at the EM level will be required to determine whether OXT molecules are attached to the outer surface of the cilia and to determine whether staining is found associated with kinocilia, stereocilia or both. The patchy distribution of parvalbumin immunofluorescence along the length of the cilia suggests that this peptide is localized within the cilia, but EM immunocytochemistry will also be required to assess its localization. Although VP-immunoreactive fibers were found in the same region of the 3V wall as OXT fibers, VP was not detected in the cilia, nor was the calcium-binding protein calbindin (Fig. 2E, 2F). The cilia were virtually translucent and very difficult to detect in sections stained for either of these proteins.

Levels of both OXT and parvalbumin immunoreactivity in the cilia were altered by light exposure at ZT23, with retinal illumination dramatically increasing OXT and decreasing parvalbumin immunoreactivity. The fact that parvalbumin levels in the 3V wall adjacent to the cilia were not altered significantly by retinal illumination suggests specific regulation of these proteins associated with the cilia.

The concomitant increase in OXT and decrease in parvalbumin levels in the cilia suggests a light-regulated mechanism for increasing the rate of distribution of OXT through the CSF. The beating motion of cilia has been proposed to serve a role in the distribution and circulation of the contents of the CSF (Roth et al., 1985), and higher levels of intracellular free calcium cause an increase in ciliary beat frequency (Nguyen et al., 2001). Since parvalbumin sequesters free calcium (Baimbridge et al., 1992), its reduction in the cilia by light exposure may increase free calcium, thereby increasing ciliary beat frequency (Nguyen et al., 2001). Since light exposure simultaneously increases OXT staining and decreases parvalbumin levels

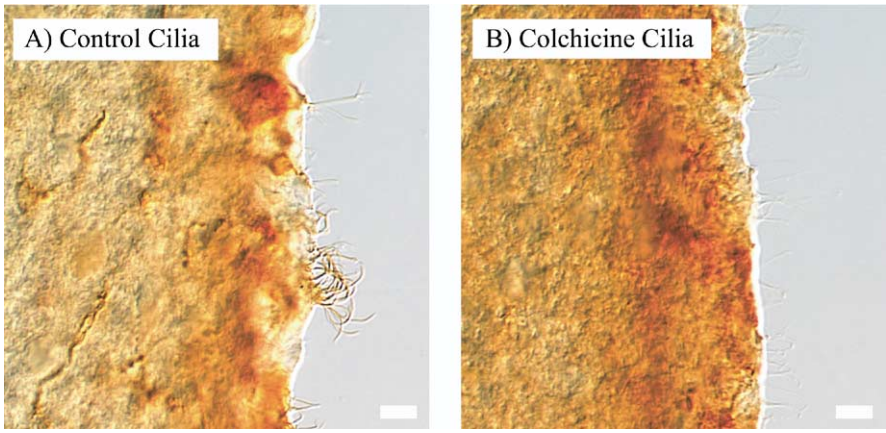


**Fig. 6.** OXT immunoreactivity in tissue from mice killed in darkness at ZT8, 24 h after i.c.v. administration of vehicle (A) or colchicine (B). Colchicine pretreatment drastically reduced the mean area of OXT staining in the cilia. Scale bar=0.01 mm in each panel.

associated with the cilia, the result would be increased levels of OXT and its more rapid circulation throughout the CSF. This would provide a mechanism, in addition to point-to-point projections from OXT neurons, for OXT to exert effects on a broad array of neural targets via the CSF.

Light exposure at night (ZT23), but not during the day (ZT8), increased OXT immunoreactivity in the 3V/AH region, but did not significantly alter OXT immunoreactivity in the neural plexus lining the 3V wall nor in the PVN. Thus, the response of OXT immunoreactivity to light exposure depended on daily phase of treatment and on the target tissue studied. The diffusely immunoreactive neural plexus only showed a significant difference in OXT levels between ZT23 and ZT8 after light exposure (Fig. 4A). If OXT levels in this region vary spontaneously at these phases, the differences were too small to detect with these methods. The method used to measure OXT immunoreactivity in the PVN was adequate to detect large changes in immunoreactivity, such as that elicited by colchicine pretreatment, but any effects of light exposure might have been too subtle to detect.

Levels of OXT, assessed as the optical density of magnocellular neurons, showed a daily rhythm in the absence of light exposure. This rhythm peaked in the PVN, neural plexus and 3V/AH during the daily dark phase (ZT16), with a trough near the beginning of the projected light phase (ZT0 or ZT4). Whether this rhythm is reflected in a daily rhythm in OXT levels in CSF in mice remains to be determined. Previous studies have reported daily rhythms in CSF OXT in rhesus macaque monkeys, but with peak levels occurring during the light phase of a daily light/dark cycle, or the subjective day under constant conditions (Artman et al., 1982; Reppert et al., 1983). The timing difference may reflect the difference in rhythm phenotype (since macaques are diurnally active while mice are nocturnal), or the endpoint measured. The limited evidence available indicates that the CSF OXT rhythm is independent of the SCN, unlike, for example, a similar daily rhythm in CSF VP levels (Reppert et al., 1983).

In early studies in rodents, no CSF OXT rhythm was reported, although constant light exposure caused a slight increase in CSF OXT (Mens et al., 1982; Reppert et al., 1983). We recently described an OXT (OXT) rhythm in the CSF of rats with higher values at ZT23 than at ZT8 (Devarajan and Rusak, 2004), opposite to that of macaques, and therefore consistent with a relationship to rhythm phenotype. This day-night difference in OXT in rat CSF is similar to the day-night difference in OXT in mouse hypothalamic tissue, but opposite to the OXT immunoreactivity rhythm in mouse 3V cilia (see above). One possibility is that cilia bind and retain OXT during the day (resulting in high levels associated with the cilia at ZT8) and release OXT into the CSF during the night (resulting in low cilia levels at ZT23). A convincing integration of these results will require direct comparisons of these measures in rats and mice.

We did not attempt to assess whether there is a spontaneous rhythm of OXT immunoreactivity in the cilia for technical reasons. To maximize detectability of OXT immunoreactivity in the AH and PVN, we sectioned the tissue with a vibratome rather than a cryostat, since freezing reduced staining intensity. Vibratome sectioning, however, tended to damage the cilia, making it impossible to evaluate staining in the cilia in this study.

Light exposure and other external stimuli can alter hormone levels in both the peripheral circulation and the CSF (Reppert et al., 1981; Seckl and Lightman, 1987a). These changes are not always parallel (Harris et al., 1981; Seckl and Lightman, 1987b), and stimuli, such as nursing, that affect circulating OXT may not similarly alter CSF levels. Our results demonstrate a mechanism by which circadian phase and retinal illumination could influence CSF OXT in mice by affecting levels of both OXT and parvalbumin associated with 3V cilia, but light-induced or circadian changes in either CSF or circulating OXT levels in mice have yet to be demonstrated.

Retinal afferents reach the region of the 3V in mice directly (Cassone et al., 1988) and the retinorecipient SCN projects to the periventricular region (Watts et al., 1987; Abrahamson and Moore, 2001), so mechanisms exist for photic input to affect cells in this region. It is, however, also possible that the effects of light exposure were mediated

indirectly by their effects on behavior. Light exposure at night may, for example, be a stressful event for a nocturnal rodent, so it would be of interest to assess whether other environmental stressors also affect the physiology of 3V cilia in a similar way (Iványi et al., 1991).

OXT transported via the CSF may alter the physiology of a number of neural systems adjacent to the brain's ventricular system and the spinal canal, since OXT receptors are very widely distributed (Gimpl and Farenholz, 2001; Tribollet et al., 1992). This route permits OXT to reach a number of neural targets rapidly and efficiently in response to environmental inputs. A broad array of functions has been attributed to OXT, including effects on maternal behavior, memory, mood and affiliative behavior (Gimpl and Farenholz, 2001). OXT has also been implicated in human depression and may contribute to the efficacy of selective serotonin reuptake inhibitor treatments (Frasch et al., 1995; Uvnäs-Moberg, 1999). Alterations of OXT levels may affect mood directly or indirectly by altering social behaviors that may be dysregulated in mood disorders (Carter et al., 1997; Uvnäs-Moberg, 1997).

Timed light exposure has been shown to improve mood in seasonal affective disorder (Rosenthal et al., 1985a,b; Terman et al., 2001) and has been proposed as a treatment for other mood disorders (Kripke et al., 1992; Pearlstein and Steiner, 2000). Similarly, increased light exposure may have a general mood-enhancing effect on humans in some situations, even in the absence of a clinical condition (Partonen and Lonnqvist, 2000). The potent regulation by light exposure of OXT levels in the hypothalamus, in the 3V cilia, and possibly in the CSF, may be one mechanism by which light can contribute to a therapeutic effect. Future research should assess whether OXT levels in 3V cilia and in CSF are regulated similarly in diurnal and nocturnal species, and whether OXT has similar effects on mood in different species.

*Acknowledgments—We would like to thank Kazue Semba, Sue Carter and David Hopkins for their valuable advice and assistance. We are also grateful to Donna Goguen, Debbie Fice, Marc Goguen, Stephen Whitefield and Haiyun Zhang for their technical assistance. Supported by grants from the Canadian Institutes of Health Research (MOP53347) and NSERC of Canada (A0305). K.D. and E.M. were supported by undergraduate and postdoctoral awards from NSERC.*

## REFERENCES

Abrahamson EE, Moore RY (2001) Suprachiasmatic nucleus in the mouse: retinal innervation, intrinsic organization and efferent projections. Brain Res 916:172–191.

Akmayev IG, Popov AP (1977) Morphological aspects of the hypothalamic-hypophyseal system. VII. The tanycytes: Their relation to the hypophyseal adrenocorticotrophic function. An ultrastructural study. Cell Tissue Res 180:263–282.

Altman J, Bayer SA (1978) Development of the diencephalon in the rat. III. Ontogeny of the specialized ventricular linings of the hypothalamic third ventricle. J Comp Neurol 182:995–1015.

Artman HG, Reppert SM, Perlow MJ, Swaminathan S, Oddie TH, Fisher DA (1982) Characterization of the daily oxytocin rhythm in primate cerebrospinal fluid. J Neurosci 2:598–603.

Aughsteen AA (2001) The ultrastructure of primary cilia in the endocrine and excretory ducts of the pancreas of mice and rats. Eur J Morphol 39:277–283.

Baimbridge KG, Celio MR, Rogers JH (1992) Calcium-binding proteins in the nervous system. Trends Neurosci 15:303–308.

Bleier R (1975) Surface fine structure of supraependymal elements and ependyma of hypothalamic third ventricle of mouse. J Comp Neurol 161:555–567.

Bruni JE (1974) Scanning and transmission electron microscopy of the ependymal lining of the third ventricle. Can J Neurol Sci 1:59–73.

Bruni JE, Del Bigio MR, Clattenburg RE (1985) Ependyma: normal and pathological. A review of the literature. Brain Res Rev 9:1–19.

Bruni JE, Montemurro DG, Clattenburg RE, Singh RP (1972) A scanning electron microscopic study of the ependymal surface of the third ventricle of the rabbit, rat, mouse and human brain. Anat Rec 174:407–420.

Carter CS, Lederhendler I, Kirkpatrick B (1997) The integrative neurobiology of affiliation. Introduction. Ann NY Acad 807:xiii–xviii.

Cassone VM, Speh JC, Card JP, Moore RY (1988) Comparative anatomy of the mammalian hypothalamic suprachiasmatic nucleus. J Biol Rhythms 3:71–91.

Celio MR (1990) Calbindin D-28k and parvalbumin in the rat nervous system. Neuroscience 35:375–475.

Choudhury SR, Azzam NA, Donohue JM (1979) Changes in the surface fine structure of rat third ventricular ependyma following chronic acetazolamide treatment. J Anat 129:51–62.

Choudhury SR, Ray PK (1990) Vasopressinergic neurons in periependymal and periventricular areas of the rostral third ventricle of the rat. Histol Histopathol 5:337–342.

Chung K, Lee WT (1988) Vasoactive intestinal peptide (VIP) immunoreactivity in the ependymal cells of the rat spinal cord. Neurosci Lett 95:1–6.

Cloft HJ, Mitchell JA (1994) Immunocytochemical detection of oxytocin in the supraependymal neuronal complex of the golden hamster. Brain Res 639:233–239.

Cougnon-Aptel N, Whiteside GT, Munglani R (1999) Effect of colchicine on neuropeptide Y expression in rat dorsal root ganglia and spinal cord. Neurosci Lett 259:45–48.

Daan S, Pittendrigh CS (1976) A functional analysis of circadian pacemakers in nocturnal rodents. II. The variability of phase response curves. J Comp Physiol 106:253–266.

Devarajan K, Rusak B (2004) Oxytocin levels in the plasma and cerebrospinal fluid of male rats: effects of circadian phase, light and stress. Neurosci Lett 367:144–147.

Edery I (2001) Circadian rhythms in a nutshell. Physiol Genomics 3:59–74.

Egli M, Bertram R, Sellix MT, Freeman ME (2004) Rhythmic secretion of prolactin in rats: action of oxytocin coordinated by vasoactive intestinal polypeptide of suprachiasmatic nucleus origin. Endocrinology 145:3386–3394.

Ekblad E, Mulder H, Sundler F (1996) Vasoactive intestinal peptide expression in enteric neurons is upregulated by both colchicine and axotomy. Regul Pept 63:113–121.

Frasch A, Zetzsche T, Steiger A, Jirikowski GF (1995) Reduction of plasma oxytocin levels in patients suffering from major depression. Adv Exp Med Biol 395:257–258.

Gaykema RPA, Zaborszky L (1997) Parvalbumin-containing neurons in the basal forebrain receive direct input from the substantia nigra-ventral tegmental area. Brain Res 747:173–179.

Gimpl G, Farenholz F (2001) The oxytocin receptor system: structure, function and regulation. Physiol Rev 81:629–683.

Harris MC, Jones PM, Robinson IC (1981) Differences in the release of oxytocin into the blood and cerebrospinal fluid following hypothalamic and pituitary stimulation in rats. J Endocrinol 157:251–257.

Hsu SM, Raine L, Fanger H (1981) Use of avidin-biotin-peroxidase complex (ABC) in immunoperoxidase techniques: a comparison

between ABC and unlabeled antibody (PAP) procedures. J Histochem Cytochem 29:577–580.
Insel TR, Gingrich BS, Young LJ (2001) Oxytocin: who needs it? Prog Brain Res 133:59–66.
Iványi T, Weigant VM, de Weid D (1991) Differential effects of emotional and physical stress on the central and peripheral secretion of neurohypophysial hormones in male rats. Life Sci 48:1309–1316.
Johnson RF, Moore RY, Morin LP (1988) Retinohypothalamic projections in the hamster and rat demonstrated using cholera toxin. Brain Res 462:301–312.
Ju G, Ma D, Duan XQ (1992) Third ventricular subependymal oxytocin-like immunoreactive neuronal plexus in the rat. Brain Res Bull 28:887–896.
Kripke DF, Mullaney DJ, Klauber MR, Risch SC, Gillin JC (1992) Controlled trial of bright light for nonseasonal major depressive disorders. Biol Psychiatry 31:119–134.
Kuchler-Bopp S, Ittel ME, Dietrich JB, Reeber A, Zaepfel M, Delaunoy JP (1998) The presence of transthyretin in rat ependymal cells is due to endocytosis and not synthesis. Brain Res 793:219–230.
Larsen PJ, Hay-Schmidt A, Vrang N, Mikkelsen JD (1996) Origin of projections from the midbrain raphe nuclei to the hypothalamic paraventricular nucleus in the rat: a combined retrograde and anterograde tracing study. Neuroscience 70:963–988.
Leah JD, Herdegen T, Murashov A, Dragunow M, Bravo R (1993) Expression of immediate early gene proteins following axotomy and inhibition of axonal transport in the rat central nervous system. Neuroscience 57:53–66.
Li Y, Stern JE (2004) Activation of postsynaptic GABAB receptors modulate the firing activity of supraoptic oxytocin and vasopressin neurones: role of calcium channels. J Neuroendocrinol 16:119–130.
Lorez HP, Richards JG (1982) Supra-ependymal serotoninergic nerves in the mammalian brain: morphological, pharmacological and functional studies. Brain Res Bull 9:727–741.
Luiten PG, Room P, Lohman AH (1980) Ependymal tanycytes projecting to the ventromedial hypothalamic nucleus as demonstrated by retrograde and anterograde transport of HRP. Brain Res 193:539–542.
Meijer JH, Rusak B, Harrington ME (1989) Photically responsive neurons in the hypothalamus of a diurnal ground squirrel. Brain Res 501:315–323.
Meijer JH, Rietveld WJ (1989) Neurophysiology of the suprachiasmatic circadian pacemaker in rodents. Physiol Rev 69:671–707.
Mens WB, Andringa-Bakker EA, Van Wimersma Greidanus TB (1982) Changes in cerebrospinal fluid levels of vasopressin and oxytocin of the rat during various light-dark regimes. Neurosci Lett 34:1–56.
Millhouse OE (1971) A Golgi study of third ventricle tanycytes in the adult rodent brain. Z Zellforsch Mikrosk Anat 121:1–13.
Moore RY (1983) Organization and function of a central nervous system oscillator: the suprachiasmatic nucleus. Fed Proc 42:2783–2789.
Muschol M, Salzberg BM (2000) Dependence of transient and residual calcium dynamics on action-potential patterning during neuropeptide secretion. J Neurosci 20:6773–6780.
Nguyen T, Chin WC, O'Brien JA, Verdugo P, Berger AJ (2001) Intracellular pathways regulating ciliary beating of rat brain ependymal cells. J Physiol 531:131–140.
Partonen T, Lonnqvist J (2000) Bright light improves vitality and alleviates distress in healthy people. J Affect Disord 57:55–61.
Pearlstein T, Steiner M (2000) Non-antidepressant treatment of premenstrual syndrome. J Clin Psychiatry 61(Suppl 12):22–27.
Porges SW (2003) Social engagement and attachment: a phylogenetic perspective. Ann N Y Acad Sci 1008:31–47.
Razzoli M, Cushing BS, Carter CS, Valsecchi P (2003) Hormonal regulation of agonistic and affiliative behavior in female mongolian gerbils (Meriones unguiculatus). Horm Behav 43:549–553.
Reppert SM, Perlow MJ, Tamarkin L, Orloff D, Klein DC (1981) The effects of environmental lighting on the daily melatonin rhythm in primate cerebrospinal fluid. Brain Res 223:313–323.
Reppert SM, Schwartz WJ, Artman HG, Fisher DA (1983) Comparison of the temporal profiles of vasopressin and oxytocin in the cerebrospinal fluid of the cat, monkey and rat. Brain Res 261:341–345.
Rosenthal NE, Sack DA, James SP, Parry BL, Mendelson WB, Tamarkin L, Wehr TA (1985a) Seasonal affective disorder and phototherapy. Ann N Y Acad Sci 453:260–269.
Rosenthal NE, Sack DA, Carpenter CJ, Parry BL, Mendelson WB, Wehr TA (1985b) Antidepressant effects of light in seasonal affective disorder. Am J Psychiatry 142:163–170.
Roth Y, Kimhi Y, Edery H, Aharonson E, Priel Z (1985) Ciliary motility in brain ventricular system and trachea of hamsters. Brain Res 330:291–297.
Rusak B, Zucker I (1979) Neural regulation of circadian rhythms. Physiol Rev 59:449–526.
Seckl JR, Lightman SL (1987a) Effect of naloxone on oxytocin and vasopressin release during vaginocervical stimulation in the goat. J Endocrinol 115:317–322.
Seckl JR, Lightman SL (1987b) Diurnal rhythm of vasopressin but not of oxytocin in the cerebrospinal fluid of the goat: lack of association with plasma cortisol rhythm. J Endocrinol 114:477–482.
Terman JS, Terman M, Lo ES, Cooper TB (2001) Circadian time of morning light administration and therapeutic response in winter depression. Arch Gen Psychiatry 58:69–75.
Tribollet E, Dubois-Dauphin M, Dreifuss J, Barberris C, Jard S (1992) Oxytocin receptors in the central nervous system. Distribution, development and species differences. Ann N Y Acad Sci 652:29–38.
Uvnäs-Moberg K (1997) Oxytocin linked antistress effects: the relaxation and growth response. Acta Physiol Scand Suppl 640:38–42.
Uvnäs-Moberg K (1999) Oxytocin as a possible mediator of SSRI-induced antidepressant effects. Psychopharmacology 142:95–101.
Vigh B, Vigh-Teichmann I (1992) Cytochemistry of CSF-contacting neurons and pinealocytes. Prog Brain Res 91:299–306.
Vigh B, Vigh-Teichmann I (1998) Actual problems of the cerebrospinal fluid-contacting neurons. Microsc Res Tech 41:57–83.
Watanabe M, Sakuma Y, Kato M (2004) High expression of the R-type voltage-gated Ca2+ channel and its involvement in Ca2+-dependent gonadotropin-releasing hormone release in GT1-7 cells. Endocrinology 145:2375–2383.
Watts AG, Swanson LW, Sanchez-Watts G (1987) Efferent projections of the suprachiasmatic nucleus: I. Studies using anterograde transport of Phaseolus vulgaris leucoagglutinin in the rat. J Comp Neurol 258:204–229.
Winslow JT, Insel TR (2004) Neuroendocrine basis of social recognition. Curr Opin Neurobiol 14:248–253.
Zahm DS, Grosu S, Irving JC, Williams EA (2003) Discrimination of striatopallidum and extended amygdala in the rat: a role for parvalbumin immunoreactive neurons? Brain Res 978:141–154.

*(Accepted 15 April 2005)*
*(Available online 20 June 2005)*